Cell, Volume *135*

Supplemental Data

A Translational Profiling Approach

for the Molecular Characterization

of CNS Cell Types

Myriam Heiman, Anne Schaefer, Shiaoching Gong, Jayms D. Peterson, Michelle Day, Keri E. Ramsey, Mayte Suárez-Fariñas, Cordelia Schwarz, Dietrich A. Stephan, D. James Surmeier, Paul Greengard, and Nathaniel Heintz

Supplemental Experimental Procedures

TRAP translational profiling

An additional point in considering the validity of the TRAP translational profiling methodology is that it makes use of BAC genetic targeting of the EGFP-L10a fusion protein to the cell type of interest. In the case of these and other BAC transgenic mice, other genes present on the BACs employed may be over-expressed, and the random insertion of the BAC DNA into the genome could conceivably result in phenotypic changes. In the case of our bacTRAP mice, our data reveal that the *Sfxn1* and *Ttc12* genes, which happen to be located on the *Drd1a* and *Drd2* BACs used, respectively, are overexpressed in the corresponding bacTRAP lines (and subsequently appear as enriched in either *Drd1a* or *Drd2* cells; see Table S2). However, we observed no phenotypic effects in the bacTRAP mice. This is not surprising given that phenotypic effects that are reproducible between lines (and therefore due to genes present on the BAC) are exceedingly rare in BAC transgenic EGFP reporter lines (GENSAT project, unpublished data), presumably because the genes carried on the BACs are only mildly over-expressed. Given these considerations, and the very high percentage of striatally enriched mRNAs that could be successfully predicted from the analysis of pooled MSN bacTRAP data, we conclude that bacTRAP data collected here reflects the normal physiological states of the MSN populations.

Another additional point in considering the validity of the TRAP methodology is that the precision of the translational profiles obtained in TRAP studies reflects both the specificity of expression of the BAC transgene, and accuracy of any gross dissections required for the desired analysis. For example, the *Drd1a* gene (Gaspar et al., 1995) and *Drd1a* BAC driver (http://www.gensat.org) are both expressed in cortical neurons in addition to striatonigral MSNs. As a result, it is possible that during rapid, manual dissection of the striatum, small amounts of contaminating cortical tissue can be inadvertently included in samples. Consequently, a small fraction of the genes present on the striatonigral-enriched gene list could conceivably represent mRNAs expressed in *Drd1a*-expressing deep layer cortical cells, depending upon the precision of dissection.

bacTRAP mice

For the striatonigral and striatopallidal bacTRAP lines, seven adult bacTRAP mice (four female, three male) were pooled for each replicate. Each cell population and pharmacological treatment was assayed in triplicate. Striatal tissue was taken between 7-9 weeks of age from CP73 (*Drd1a*/EGFP-L10a) and CP101 (*Drd2*/EGFP-L10a) mice. All mice were raised under 12h dark/12h light conditions, housed 5 mice per cage, with

food and water *ad libitum*. All mice used in the study were heterozygous for the EGFP-L10a transgene; mice from each line had been crossed to wild-type Swiss-Webster (Taconic Farms) four times. All animal use protocols were approved by the Rockefeller University Institutional Animal Care and Use Committee. Mice used for the baseline comparison of *Drd1a* versus *Drd2* cells were used directly from the home cage. For all cocaine studies, bacTRAP mice 7-9 weeks of age were singly housed and intraperitoneally injected at the Rockefeller University Laboratory Animal Research Center (LARC) and were moved to the laboratory approximately 16 h before the final injection. For acute cocaine studies, all mice were injected with 100 µl saline (vehicle) once daily for eight days to habituate the mice to handling. On the ninth day mice were injected with a test dose of 20 mg/kg cocaine or 100 µl saline and the striata were harvested 4 h after this test injection. For chronic cocaine studies, mice were injected with 20 mg/kg cocaine or 100 µl saline once daily for fifteen days and the striata were harvested 4 h after the last injection.

bacTRAP purifications from *Chat* and *Pcp2* lines

For the purification of translated mRNAs from brain stem cholinergic motor neurons (from the *Chat* bacTRAP line) or cerebellar Purkinje neurons (from the *Pcp2* bacTRAP line), nearly identical purifications to those outlined in the main experimental procedures section for the striatonigral and striatopallidal lines were performed, with the exception that two mouse anti-EGFP monoclonal antibodies (described in the accompanying paper, Doyle, Dougherty, et al., 2008) were used in the immunoprecipitations instead of a goat anti-EGFP antibody. Brainstems from three adult *Chat* bacTRAP mice were pooled; cerebellums from three adult *Pcp2* bacTRAP mice were pooled (in each case males and females were used, evenly balanced across replicates). For the dissection of the cerebellum in *Pcp2* bacTRAP studies, the cerebellum was removed by cutting at the peduncles. For the dissection of the brain stem in *Chat* bacTRAP studies, the brainstem was first cut from the spinal cord at the level of the foramen magnum. The cerebellum was then removed by cutting the peduncles. Anteriorly, an incision was made from just rostral to the colliculi (dorsally) to the junction between the hypothalamus and the pons (ventrally), so as to include the occulomotor nuclei. This dissection includes all cholinergic motor neurons above the spinal cord, as well as the more weakly labeled cholinergic neurons of the pedunculopontine and laterodorsal tegmental nuclei (PPT/LDT).

Quantitation and amplification of mRNA samples

Purified mRNA samples were analyzed using a Bioanalyzer (Agilent Technologies, Santa Clara, CA) in order to assess mRNA quantity and quality, as reflected by rRNA levels and integrity. Purified RNA was converted to double-stranded cDNA using the SuperScript GeneChip Expression 3'-Amplification Reagents Two-Cycle cDNA Synthesis Kit (Affymetrix, Santa Clara, CA) and the GeneChip T7-Oligo(dT) Primer (Affymetrix, Santa Clara, CA). cDNA was used for the *in vitro* synthesis of cRNA using the MEGAscriptT7 Kit (Ambion, Austin, TX). cRNA was purified using the GeneChip Sample Cleanup Module (Affymetrix, Santa Clara, CA). 600ng or less of clean cRNA was used in the second-cycle cDNA synthesis reaction using the SuperScript GeneChip Expression 3'-Amplification Reagents Two-Cycle cDNA Synthesis Kit (Affymetrix, Santa Clara, CA) and random primers (Affymetrix, Santa Clara, CA). The cDNA was purified using the GeneChip Sample Cleanup Module (Affymetrix, Santa Clara, CA). Purified cDNA was used for the *in vitro* synthesis of biotin-labeled cRNA using the GeneChip IVT Labeling Kit (Affymetrix, Santa Clara, CA). cRNA was purified using the GeneChip

Sample Cleanup Module (Affymetrix, Santa Clara, CA) and fragmented into 35-200 base pair fragments using a magnesium acetate buffer (Affymetrix, Santa Clara, CA). Ten micrograms of labeled cRNA were hybridized to Affymetrix GeneChip Mouse Genome 430 2.0 arrays (http://www.affymetrix.com/products/arrays/specific/mouse430_2.affx) for 16 h at 45ºC. The GeneChips were washed and stained according to the manufacturer's recommendations (Affymetrix, Santa Clara, CA) using the GeneChips Fluidics Station 450 (Affymetrix, Santa Clara, CA). Mouse Genome 430 2.0 arrays were scanned using the GeneChip Scanner 3000 (Affymetrix, Santa Clara, CA).

Microarray data normalization and analysis

Three biological replicates were performed for each experiment. Quantitative PCR reactions were performed to validate array results using an independent biological source and amplification methodology (see **Quantitative PCR** section below). GeneChip CEL files were subjected to Harshlight analysis to detect if any blemishes were present on the GeneChips (http://asterion.rockefeller.edu/Harshlight/index2.html) (Suarez-Farinas et al., 2005). Only GeneChips without major blemishes were used. Striatonigral and striatopallidal GeneChip CEL files were imported into Genespring GX 7.3.1 (Agilent Technologies, Santa Clara, CA), processed with the GC-RMA algorithm, and expression values on each chip were normalized to that chip's 50th percentile. Data were converted to $\log_2$ scale and filtered to eliminate genes with intensities in the lower range. Only genes where more than one sample had a normalized intensity larger than 16 (4 in $\log_2$ scale) were kept in the analysis. Statistical analysis to determine which genes are differentially expressed in the different conditions was carried out using the Limma package from Bioconductor project (http://www.bioconductor.org). For the baseline comparison of striatonigral versus striatopallidal cells, a moderated two-tailed paired t-test was performed. The p-value of the moderated t-test was adjusted for multiple hypothesis testing, controlling the false discovery rate (FDR) using the Benjamini-Hochberg procedure. We then selected all genes that had an FDR less than 0.1 (10%) and fold change larger than 1.5.

Upon clustering, all cocaine data exhibited a strong effect of the day the samples were prepared (data not shown). This led us to consider a more complex analysis model that could take into account and adjust for this day effect. A linear model was adjusted to each gene with factor Treatment (Saline vs Cocaine), Cell type (*Drd1a* vs *Drd2*), and Day (three different days for acute and chronic experiments). With this analysis, a large number of genes indeed displayed a significant Day factor. With this model fitted, we were able to test all the hypotheses of interest (Cocaine vs Saline and its interaction with Cell type in both Acute and Chronic). For assessing differential expression in the comparisons of interest, the moderated t-statistic was used (Smyth, 2004). In this assessment, an empirical Bayes method is used to moderate the standard errors of the estimated $\log_2$-fold changes. This method was particularly useful for our analysis with only three replicates of each condition, as it delivered more stable inference and improved power. The p-value of the moderated t-test was adjusted for multiple hypothesis testing, controlling the false discovery rate (FDR) using the Benjamini-Hochberg procedure. We then selected all genes than have FDR less than 0.1 (10%) and fold change larger than 1.4.

For the comparison of striatonigral and striatopallidal bacTRAP samples versus total brain minus striatum, GeneChip CEL files were imported into Genespring GX 7.3.1, normalized with the GC-RMA algorithm (bacTRAP samples and whole brain minus striatum samples separately), and expression values on each chip were further normalized to the expression values of several positive control genes and to a constant

value of 0.01. After conversion to $\log_2$ scale, data was filtered to eliminate genes with intensities in the lower range as above, and a moderated two-tailed t-test was performed. The p-value of the moderated t-test was adjusted for multiple hypothesis testing, controlling the false discovery rate (FDR) using the Benjamini-Hochberg procedure. We then selected all genes that had an FDR less than 0.05 (5%) and fold change larger than 2.

For the comparison of bacTRAP IP samples versus a common reference sample (IP versus reference), each group of replicate IP datasets (*Drd1a*, *Drd2*, *Chat*, and *Pcp2*) were imported individually into Genespring 7.3.1 and normalized with the GC-RMA algorithm. Array datasets from 12 unbound samples of the purifications (3 unbound replicates per *Drd1a*, *Drd2*, *Chat*, and *Pcp2*) were imported together into Genespring 7.3.1 and normalized with the GC-RMA algorithm to make a common 'reference' sample. Each dataset (*Drd1a*, *Drd2*, *Chat*, *Pcp2*, and 'reference;' each now containing averaged data from constituent replicates) was then further normalized to Affymetrix biotin spike-in probes and then divided by 0.002 for scaling purposes. A gene list was made of all probes present on the arrays minus a few contaminating probes found to be consistently non-specifically purified (Supplemental Table 2 of the accompanying paper, Doyle, Dougherty, et al., 2008). For each IP dataset, a list of 'expressed' probesets was generated (normalized expression >50) from the list of all genes minus contaminating probes. Each IP dataset was then individually compared to the 'reference' sample, and the top 1,000 IP-enriched probesets from each 'expressed' list were selected. Finally, these lists were compared by Venn diagrams. In order to generate scatterplots for these IP versus reference comparisons, datasets were normalized as above, except that these steps were identically performed in the program R. Probesets were plotted if they had an average expression >100.

To translate the mRNA translation data into functional profiles, we used Gene Ontology (GO) analysis and Pathway analysis to look for enriched GO terms and Pathways in the set of differentially expressed genes. Analysis of GO annotations was performed using the R-packages GOstats and GOtools. To find those GO terms that were over-represented in the list of genes in question, for each specific term in a given ontology (Biological Process, Molecular Function, Cellular Component), the proportion of genes in the list that falls into the GO term is compared with the proportion in the whole set of genes in the Mouse Genome 430 2.0 array using a conditional hypergeometric test. We used a conditional instead of the classical hypergeometric test to address concerns about the hierarchical structure of GO terms (Alexa et al., 2006; Falcon and Gentleman, 2007). The conditional test uses the relationship among GO terms to decorrelate results. GO with p-values < 0.1 and with more than one gene were considered. To find overrepresented Pathways, we used the classical hypergeometric test to compare the proportion of genes among those that are differentially expressed (Up and Down together) that belong to a certain Pathway, using the whole Mouse Genome 430 2.0 array gene set as the universe for the comparison. A Pathways annotation package available at Bioconductor.org (version 1.16.0) was used. The KEGG Pathways terms in that package were obtained from KEGG:ftp://ftp.genome.ad.jp/pub/kegg/tarfiles/pathway.tar.gz, build release 41.1, February 1, 2007.

Polysome Profiling

Standard methods for polysome profiling were used. HEK293T cells or striata pooled from 10 mice were homogenized in lysis buffer. The solubilized and clarified lysate was loaded onto a linear density (20-50% w/w) gradient of sucrose and centrifuged for 2 hours at 4 °C using a Beckman SW41 rotor at 40,000 r. p. m. (200, 000 x *g*). 750 µl

fractions were collected as absorbance at 254 nm was monitored with an ISCO UA-6 UV detector.

Immunoblotting

Standard methods for immunoblotting were used. Antibodies were used as follows: GFP detection: JL-8, Clontech (Mountain View, CA), 1:2,000 in 5% non-fat milk/PBS-T (phosphate buffered saline-0.05% Tween-20); Rpl7 detection: NB200-308, Novus Biologicals (Littleton, CO), 1:2,000 in 5% IgG-free bovine serum albumin/PBS-T; Rpl10a detection: H00004736-M01, Abnova Corporation (Taipei City, Taiwan), 1:2,000 in 5% IgG-free bovine serum albumin/PBS-T; Ferritin detection: 65077, MP Biomedicals (Solon, OH), 1:1,500 in 0.2% I-block (Applied Biosystems, Foster City, CA)/PBS-T; β-Actin detection: Ab8224, Abcam (Cambridge, MA), 1:2,500 in 5% non-fat milk/PBS-T.

Electron Microscopy

Following immunoprecipitation, aliquots of anti-GFP coated magnetic beads were fixed in 2.5% glutaraldehyde/0.1M cacodylate [pH 7.4] on ice. The bead pellet was post-fixed with 1% osmium tetroxide in the same buffer on ice. After treatment with 0.5% aqueous uranyl acetate at room temperature, the specimen was dehydrated with graded alcohol (70, 90, 100%) and treated with propylene oxide before embedding in Embed 812 resin. The resin was polymerized in a 60 °C oven for 2-3 days. Silver sections were cut with a Dupont diamond knife on a Reichert-Jung UltraCut E ultramicrotome. The sections were collected on copper grids, doubly stained with saturated, aqueous uranyl acetate and lead citrate before examination with a Jeol 100cx electron microscope (JEOL, Peabody, MA) operated at 80kV.

Immunohistochemistry

7-9 week old bacTRAP transgenic mice were deeply anesthetized with pentobarbitol and transcardially perfused with 10ml of phosphate buffered saline (PBS) followed by 40ml of 4% paraformaldehyde (PFA) in PBS. Brains were dissected and post-fixed at room temperature for exactly 1 h with 4% PFA in PBS. Brains were washed 3 times 5 min in PBS and incubated in 5% weight/volume (w/v) sucrose in PBS at 4°C for 1 h with gentle agitation. Brains were then incubated for 24 h in 15% w/v sucrose in PBS at 4°C with gentle agitation and for 24 h in 30% w/v sucrose in PBS at 4°C with gentle agitation. Brains were placed in an embedding mold filled with Neg-50 embedding medium (Richard Allan Scientific, Kalamazoo, MI) for 1 hour at room temperature, and were subsequently incubated on dry ice for 1 hour to freeze the embedding medium. Brains were then transferred to and stored at –80°C until sectioned. 12 µm sagittal sections were cut, mounted on glass slides, and kept overnight at –20°C, then transferred to –80°C until used for immunohistochemistry. Before use sections were thawed and dried at room temperature for 20 min, washed with PBS, and incubated in 0.2%H_2O_2/PBS at room temperature for 30 min to quench endogenous peroxidase activity. Sections were washed with PBS, permeabilized with PBS/0.05%Tween-20, and blocked with Image-it FX signal enhancer (Invitrogen Corporation, Carlsbad, CA) for 30 min at room temperature. Sections were washed with PBS/0.05%Tween-20 and blocked again with 2%donkey serum/0.1%fish gelatin/PBS/0.05%Tween-20. Sections were then incubated overnight at 4°C with primary antibody against Met-enkephalin (ab22620 diluted 1:500, Abcam, Cambridge, MA) or against GFP (ab6556, diluted 1:5,000, Abcam, Cambridge, MA) diluted in 2%donkey serum/0.1%fish gelatin /PBS/0.05%Tween-20. The next day, sections were washed with PBS/0.05%Tween-20 and incubated with anti-rabbit Superpicture HRP Polymer Detection Kit (Invitrogen Corporation, Carlsbad, CA) for 1 h

at room temperature. Sections were washed with PBS/0.05%Tween-20 and a fluorescent HRP substrate, Tyramide-AlexaFluor 546 conjugate (from TSA kit #13, Invitrogen Coroporation, Carlsbad, CA), was deposited on the slides. Slides were washed again with PBS/0.05% Tween-20, mounted with Prolong Gold Antifade (Invitrogen Corporation, Carlsbad, CA), dried overnight, and fluorescence was visualized on a Zeiss LSM510 confocal microscope (Carl Zeiss, Thornwood, NY).

In Figure 2 we present colocalization data for EGFP-L10a (direct EGFP fluorescence) and pro-enkephalin expression (immunohistochemical staining). In the *Drd2* line, we observed 75.8% colocalization of pro-enkephalin with EGFP-L10a (n=204/269), and in the *Drd1a* line we observed 0% colocalization (n=0/325). For the *Drd2* line, this number is likely an underestimate, as in our experience heat-induced epitope retrieval in citrate buffer is needed for optimal staining using pro-enkephalin antibodies. We were unable to use epitope retrieval in our colocalization experiments, however, because both EGFP fluorescence and the ability of various GFP antibodies to recognize EGFP were substantially diminished upon use of these epitope retrieval methods.

Indirect Immunofluorescence

Brains were fixed and cryoprotected as above, frozen, cut to 40 μm serial floating sections on a cryostat, and stored in PBS with 0.1% sodium azide at 4°C until use. Sections were blocked in PBS with 5% normal donkey serum and 0.25% Triton X-100 for 30 minutes, then incubated overnight with primary antibodies (Choline Acetyltransferase, AB143 from Chemicon, Temecula, CA; Calbindin-D28K, Antibody 300 from Swant, Bellinzona CH; EGFP, AB19370 from Abcam, Cambridge, MA). Sections were washed in PBS, exposed to appropriate Alexa-dye conjugated secondary antibodies (Invitrogen Corporation, Carlsbad, CA) for 90 minutes, washed, and then mounted.

Quantitative PCR

20ng of purified RNA was used to produce cDNA with a NuGEN WT Ovation kit (NuGEN Technologies, San Carlos, CA) and the resulting cDNA was purified and quantitated. 10ng of cDNA was used for each real-time gene expression assay. Applied Biosystems (Foster City, CA) TaqMan pre-designed gene expression assays were used, following the manufacturer's instructions and using an Applied Biosystems 7900 Sequence Detection System. Assays used were *Gapdh*: Mm99999915_g1, *Drd2*: Mm00438541_m1, *Gpr6*: Mm01701705_s1, *Lhx8*: Mm00802919_m1, *Gpr88*: Mm02620353_s1, *Trpc4*: Mm00444284_m1, *Tpm2*: Mm00437172_g1, *Eya1*: Mm00438796_m1, *Tac1*: Mm00436880_m1, *Isl1*: Mm00627860_m1, *Gng2*: Mm00726459_s1, *Chrm4*: Mm00432514_s1, *Drd1a*: Mm02620146_s1, *Crym*: Mm01281258_m1, *Actb*: Hs99999903_m1, and *Fth1*: Hs01694011_s1. Each assay was performed in quadruplicate and fold enrichment values were derived from the comparative Ct method (following Applied Biosystems recommendations), with each target amplification compared to a *Gapdh* or *Actb* reference amplification.

Brain slice preparation for optical/electrophysiological study

Slices were obtained from 32- to 37-day-old BAC *Drd1a* or BAC *Drd2* soluble EGFP-expressing transgenic mice (Gong et al., 2003). All animals were handled in accord with Northwestern University ACUC and NIH guidelines. For chronic cocaine studies, mice were injected with 20mg/kg cocaine or 100 μl saline once daily for fifteen days and brain slices were prepared 4 h after the last injection, as in the mRNA studies. Coronal slices containing the striatum were prepared at a thickness of 250 μm. The mice were deeply

anesthetized with ketamine and xylaxine, transcardially perfused with oxygenated, ice cold, artificial cerebral spinal fluid (ACSF), and decapitated. Brains were rapidly removed and sectioned in oxygenated, ice-cold, ACSF using a Leica VT1000S vibratome (Leica Microsystems, Germany). The ACSF contained the following (in mM): 126 NaCl, 3 KCl, 2 $CaCl_2$, 1 $MgCl_2$, 25 $NaHCO_3$, 1.25 NaH_2PO_4, and 15.6 D-(+)-glucose. Unless otherwise noted, all chemicals and reagents were obtained from Sigma (St. Louis, MO). The slices were transferred to a holding chamber in which they were completely submerged in ACSF at 35°C for 1 h, after which they were stored at room temperature (22ºC–23ºC) until whole-cell recording. All ACSF solutions were bubbled continuously with 95%O_2 and 5%CO_2 to maintain oxygenation and a pH≈7.4, and periodically checked to ensure ≈300 mOsm/l.

Electrophysiological analysis of GABAergic synaptic events

Whole-cell voltage-clamp recordings were performed using standard techniques. Individual slices were transferred to a submersion-style recording chamber on an Olympus Optical (Melville, NY) BX50WI microscope and continuously superfused with ACSF at a rate of 2–3 ml/min at 22ºC–23ºC. Whole-cell voltage-clamp recordings were performed on striatal medium spiny neurons detected in the slice with the help of an infrared-differential interference contrast (IR-DIC) video microscope with an Olympus OLY-150 camera/controller system (Olympus, Japan). The following were added to the superfusion medium for all experiments to isolate mIPSCs: 50 mM 2-amino-5-phosphonopentanoic acid (AP-5, Tocris Cookson, Ellisville, MO) to block NMDA glutamate receptors, 5 mM 1,2,3,4-Tetrahydro-6-nitro-2,3-dioxo-benzo^{2}quinoxaline-7-sulfonamide (NBQX) to block AMPA/kainite glutamate receptors, and 1 mM tetrodotoxin (TTX, Alomone Labs, Jerusalem, Israel) to block sodium channels. Patch electrodes were made by pulling Sutter BF150-86-10 glass on a P-97 Flaming/Brown micropipette puller (Sutter Instrument, Novato, CA) and fire polished before recording. Pipette resistance was typically 2.5–4 MΩ after filling with an internal solution containing the following (in mM): 140 CsCl, 1.5 $MgCl_2$, 10 HEPES, 0.1 BAPTA-Cs, 5 QX-314, 2 ATP-Na_2, 0.4 GTP-Na_2, pH 7.25-7.3 adjusted with CsOH, 270-280 mOsm/L. Miniature IPSCs were recorded with a Multiclamp 700A amplifier, a Digidata 1322A 16-bit data acquisition system, and pClamp software version 8.2 (Molecular Devices, Union City, CA) in gap free mode. Neurons were voltage-clamped at -80 mV and allowed to reach a stable baseline (≈5 min) before mIPSCs were recorded for 7 min. Mini Analysis (Synaptosoft Inc., Fort Lee, NJ) was used to analyze mIPSC amplitude, frequency, 10-90% rise time, decay time, and non-stationary noise analysis. A threshold of 5 times the root mean square baseline noise level (commonly≈20-25 pA) was set for event detection. Records were then visually inspected and all events triggered by noise were discarded. Frequency analysis was carried out on all mIPSCs that met threshold criteria. Events were then selected for amplitude, 10-90% rise time, and decay time analysis on the following criteria: 1) Events with 10-90% rise times faster than 1 ms were selected to minimize space clamp errors and electrotonic filtering; 2) Events with decay times faster than 50 ms were selected to minimize events in which multiple events precluded accurate decay time measurement. For non-stationary noise analysis, the same criteria for amplitude and mIPSCs kinetics were used followed by these additional criteria: 3) No multiple events in which the decay did not return to baseline; 4) Events had to have a stable baseline before the rise and after the end of the decay. Mean values of mIPSC measures were compared between groups with a one-tailed t-test or Mann-Whitney rank sum test using Sigma Stat 3.0 (Systat Software Inc., Richmond, CA). Pooled data are presented as means ± SE and box plots using IGOR 5.00 (WaveMetrics, Lake Oswego, OR).

2-photon laser scanning microscopy (2PLSM)

Striatonigral (BAC *Drd1a*) or straitopallidal (BAC *Drd2*) neurons expressing soluble EGFP (Gong et al., 2003) in 275 µm thick corticostriatal slices were identified by somatic EGFP fluorescence. EGFP 2PLSM green signals (500-550 nm) were acquired from EGFP+ BAC *Drd2* neurons using 810 nm excitation, while EGFP+ BAC *Drd1a* neurons required 900 nm excitation. EGFP+ MSNs were then patched using infrared-differential interference contrast (IR-DIC) video microscopy with a Hamamatsu C2400 Newvicon camera/controller system (Hamamatsu, Japan) and a 60X/0.9NA water-dipping lens. Patch electrodes were made by pulling BF150-86-10 glass on a P-97 Flaming/Brown micropipette puller (both from Sutter Instrument Co., Novato, CA). The pipette solution contained the following (in mM): 135 $KMeSO_4$ (ICN Biomedicals Inc., Aurora, OH), 5 KCl, 10 HEPES, 2 MgATP, 0.2 Na_2GTP, and 0.1 spermine, pH=7.25-7.3 with KOH, 270 mOsm/l. As measured in the bath, the pipette resistance was ~4MΩ. Seals were formed in voltage-clamp mode on the cell somas with series resistance >1GΩ. After seal rupture in whole-cell configuration the series-resistance decreased to 10-15MΩ. Alexa 594 (50 µM, Ca^{2+}-insensitive red dye), for visualization of the dendrites, and Fluo-4 (200 µM, Ca^{2+}-sensitive green dye), for measuring changes in intracellular dendritic Ca^{2+}, was dissolved in the internal pipette solution. EGFP fluorescence was below our threshold for detection in the dendrites and did not contribute background signal during calcium imaging. Thapsigargin was also added to the internal solution in some experiments to block ER-mediated Ca^{2+} release. The thapsigargin was initially dissolved in DMSO at a concentration of 10 mM. This stock was then diluted 1000X in the internal recording solution. Following break in, the internal solution was allowed to approach diffusional equilibrium for at least 15 min prior to imaging. The cells were voltage clamped at –70mV and monitored for somatic depolarization.

For the duration of the recordings, 2PLSM green and red signals (570-620 nm) were acquired using 810nm excitation with 90MHz pulse repetition frequency and ~250fs pulse duration at the sample plane. A second puffer pipette containing sphingosine 1-phosphate (S1P, 10 µM) was positioned for focal dendritic application. The S1P was initially dissolved in DMSO at a concentration of 10 mM. This stock was then diluted 1000X into HEPES-buffered ACSF containing 4 mg/ml BSA, pH=7.4. Changes in dendritic Ca^{2+} were measured by acquiring high magnification maximum projection images of dendrite segments 50-100 µm from the soma. These images were acquired with 0.17 μm^2 pixels and 2.2 µs dwell time and consisted of 10-20 images taken at 0.5 µm focal steps. The change in Ca^{2+} was determined by calculating the percent change in fluorescence of the green dye normalized to the red dye ($\Delta G/R$). Following Ca^{2+} imaging, maximum projection images of the soma and dendritic field were acquired with 0.27 μm^2 pixels and 2.6 µs pixel dwell time and consisted of ~80 images taken at 0.7 µm focal steps.

The two-photon excitation source was a Chameleon-XR tunable laser system (705nm to 980nm, Coherent Laser Group, Santa Clara, CA). Laser average power attenuation was achieved with two Pockels cell electro-optic modulators (models 350-80 and 350-50, Con Optics, Danbury, CT). The two cells are aligned in series to provide enhanced modulation range for fine control of the excitation dose (0.1% steps over four decades). The laser-scanned images were acquired with a Bio-Rad Radiance MPD system (Hemel Hempstead, England, UK). The fluorescence emission was collected by external or non-de-scanned photomultiplier tubes (PMTs). The green fluorescence (500 to 550nm) was detected by a bialkali-cathode PMT and the red fluorescence (570nm to 620nm) was collected by a multi-alkali-cathode (S-20) PMT. The fluorescence was acquired in 16 bit photon counting mode. The laser light transmitted through the sample

was collected by the condenser lens and sent to another PMT to provide a bright-field transmission image in registration with the fluorescent images. The stimulation, display, and analysis software was a custom-written shareware package, WinFluor and PicViewer (John Dempster, Strathclyde University, Glasgow, Scotland; UK).

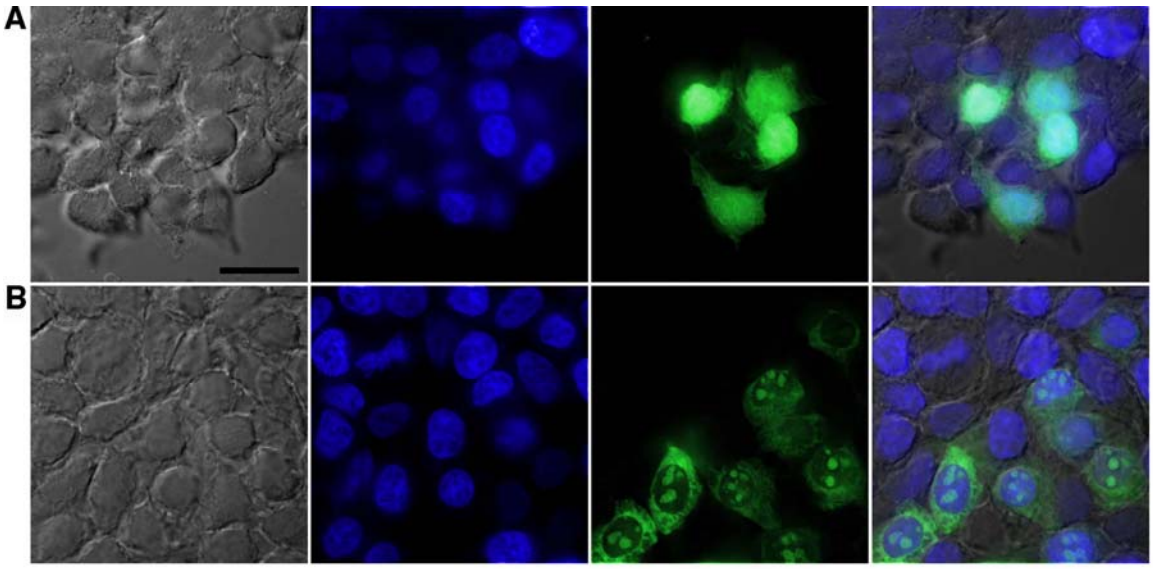

Figure S1. EGFP and EGFP-L10a expression in HEK293T cells HEK293T cells grown on coverslips were transiently transfected, grown for two days, fixed with paraformaldehyde, and mounted with media containing 4',6-diamidino-2-phenylindo (DAPI) to stain DNA. Panels from left: Differential interference contrast (DIC), DAPI, EGFP fluorescence, and merge. (A) Cells transfected with EGFP (B) or EGFP-L10a, both driven from the CMV promoter. Scale bar = 20 μm.

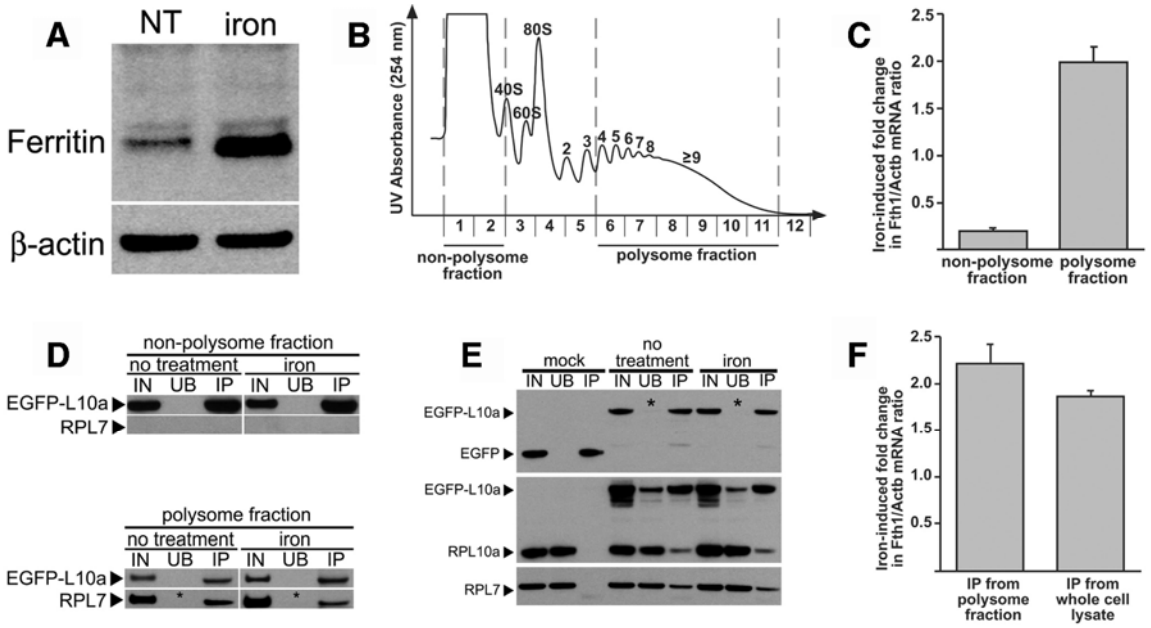

Figure S2. Immunoprecipitation of translated mRNAs from transfected cells
HEK293T cells were transiently transfected (~30% efficiency) with EGFP (mock) or EGFP-L10a constructs and grown in medium alone (no treatment, NT) or in medium supplemented with 100 µg/ml ferric ammonium citrate [pH 7.0] (iron) for 36 hours. (A) Induction of the iron-storage protein Ferritin was seen after 36 hours of iron treatment. (B) The post-mitochondrial supernatants of untreated or iron-treated cells were loaded onto linear sucrose gradients (20-50% w/w). After velocity sedimentation, fractions (direction of sedimentation noted by arrow) were collected while UV absorbance (254 nm) was being measured. A representative trace is shown, as profiles from non-treated and iron-treated lysates looked nearly identical. Non-polysome and polysome gradient fractions were generated as indicated. To avoid Ferritin mRNAs associated with mRNPs, only heavier polysomes (with greater than 4 ribosomes) were included in the polysome fraction. (C) After iron treatment, an increase in the translation efficiency of Ferritin subunit-encoding mRNAs has been reported to result from a shift of Ferritin mRNA into polysome fractions from non-polysome fractions (Rogers and Munro, 1987; Zahringer et al., 1976). As expected, we observed a shift of Ferritin heavy chain mRNA (*Fth1*) out of non-polysome fractions into polysome fractions, as determined by reverse transcription followed by quantitative PCR of total RNA purified from non-polysome and polysome gradient fractions (range of fold-change in non-polysome fraction: 0.16-0.22; range of fold-change in polysome fraction: 1.83-2.15). (D) Immunoprecipitations were performed from non-polysome or polysome gradient fractions and 0.2% of the Input (IN), 0.02% of the unbound (UB), and 1% of the bound (IP) samples were loaded onto gels for immunoblot analysis with EGFP or Rpl7 antibodies; * indicates the presence of a weak Rpl7 band upon much longer exposure. EGFP-L10a was recovered equally well from non-polysome and polysome fractions with or without iron treatment. Rpl7 was recovered equally well from untreated or iron-treated polysome fractions. Rpl7 was not present in the non-polysome fraction, presumably because, unlike the overexpressed EGFP-Rpl10a, it was all incorporated into polysomes. As expected from the lack of Rpl7 (and thus assembled ribosomes) in the non-polysome fraction, immunoprecipitations from non-polysome fractions did not pull down any RNA above background (data not shown), indicating that the immunoprecipitation was specific to translated messages. (E)

To determine if the TRAP methodology could faithfully reflect the changes observed in C, we performed direct EGFP immunoprecipitations of post-mitochondrial supernatants (whole cell lysates, unfractionated). 0.5% of input (IN), 0.5% of the unbound fraction (UB), and 1.0% of the bound (IP) samples were loaded onto gels for immunoblot analysis with EGFP (top), Rpl10a (middle), or Rpl7 (bottom) antibodies. EGFP-L10a was recovered equally well from untreated and iron-treated samples, as was all EGFP from mock samples; * indicates the presence of a light EGFP-L10a band upon longer exposure. No endogenous Rpl10a or Rpl7 was recovered in the bound (IP) fraction of mock samples, while endogenous Rpl10a and Rpl7 were both recovered in the bound (IP) fraction of untreated and iron-treated samples. The reduced recovery of endogenous Rpl10a versus endogenous Rpl7 in the immunoprecipitation likely reflects competition between endogenous Rpl10a and EGFP-L10a for incorporation into ribosomes. (F) The iron-induced fold-change in *Fth1* mRNA levels relative to *Actb* mRNA levels in samples immunoprecipitated (IP) from either polysomes or from whole cell lysates (range of fold-change in polysome IP samples: 2.01-2.43; range of fold-change in direct IP samples: 1.80-1.93) was similar to the change observed in the polysome gradient fraction before immunoprecipitation (C).

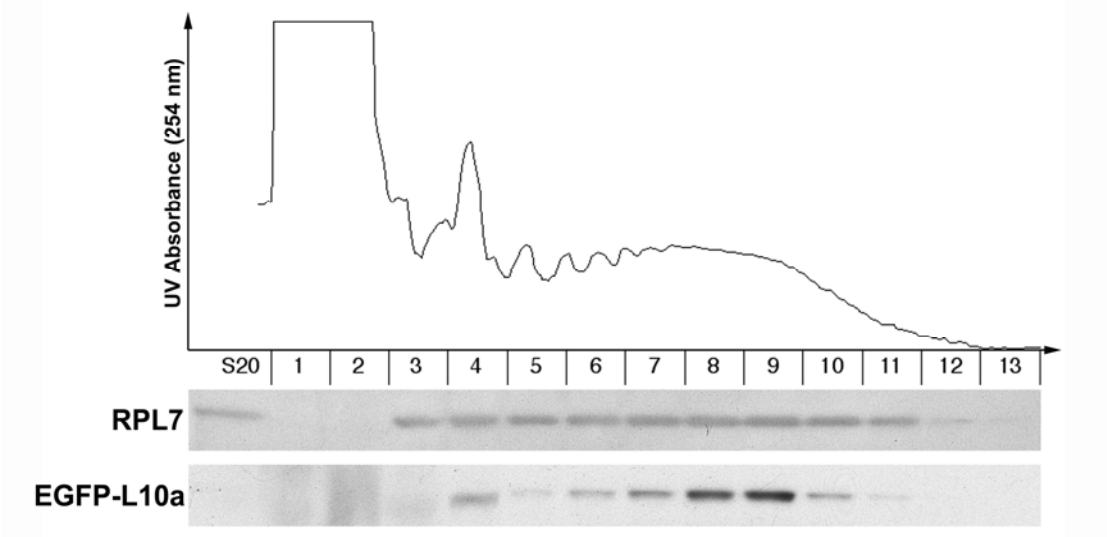

Figure S3. Polysome profile from *Drd2* bacTRAP mouse striatal extract Top: Post-mitochondrial striatal extract (S20) was loaded onto a linear sucrose gradient (20-50% w/w). After velocity sedimentation, fractions (direction of sedimentation noted by arrow) were collected as UV absorbance (254 nm) was measured. Bottom: gradient fractions were ethanol precipitated, resuspended in SDS-PAGE loading buffer, and Rpl7 and EGFP-L10a content were assayed by Western blotting.

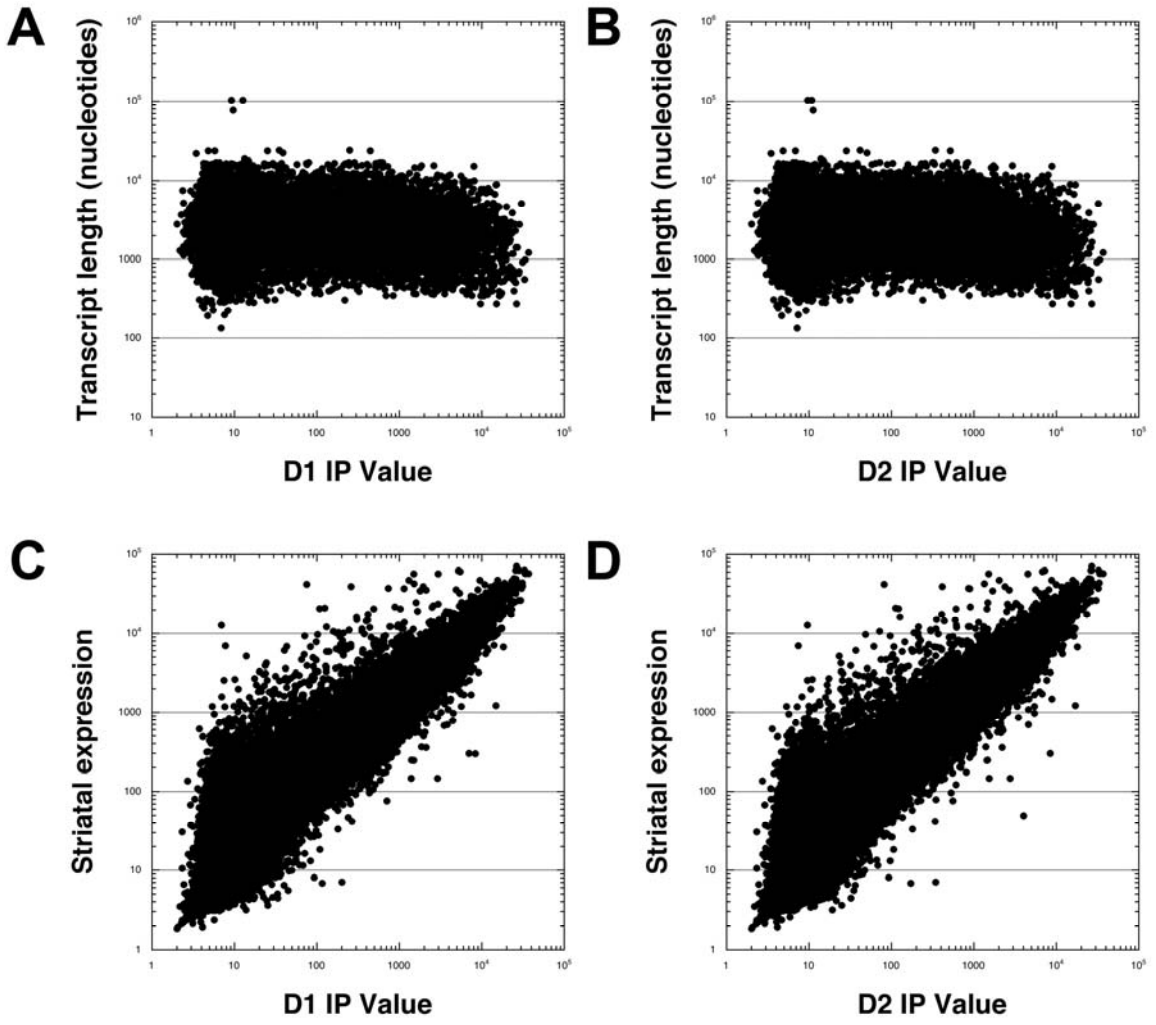

Figure S4. Analysis of striatal MSN IP values relative to message abundance and length

Lengths of transcripts were based on all available mouse curated RefSeq RNA sequences (ftp://ftp.ncbi.nih.gov/genomes/M_musculus/RNA on July 3, 2008). Where multiple transcript variants for a single gene were available, the longest one was chosen. RefSeq lengths were plotted against *Drd1a* (A) or *Drd2* (B) bacTRAP IP normalized expression values. There was no notable correlation observed between transcript length and *Drd1a* or *Drd2* IP values (Pearson correlation r = -0.08 and r = –0.07, respectively). Due to the density of datapoint overlap, particularly among the numerous <1kb transcripts, not all datapoints are discernible by eye on these log-log plots. Striatal expression values for all Affymetrix Genechip probe-sets were obtained by total RNA arrays from wild-type striatal tissue (data not shown). These values were plotted against (C) *Drd1a* bacTRAP or (D) *Drd2* bacTRAP IP normalized values. As expected, expression in total striatum (no IP, wild type mice) correlated strongly with *Drd1a* or *Drd2* bacTRAP IP values (Pearson correlation r = 0.87 for both analyses). The few genes that

show modest expression in total striatum but have low IP values include known non-neuronal genes.

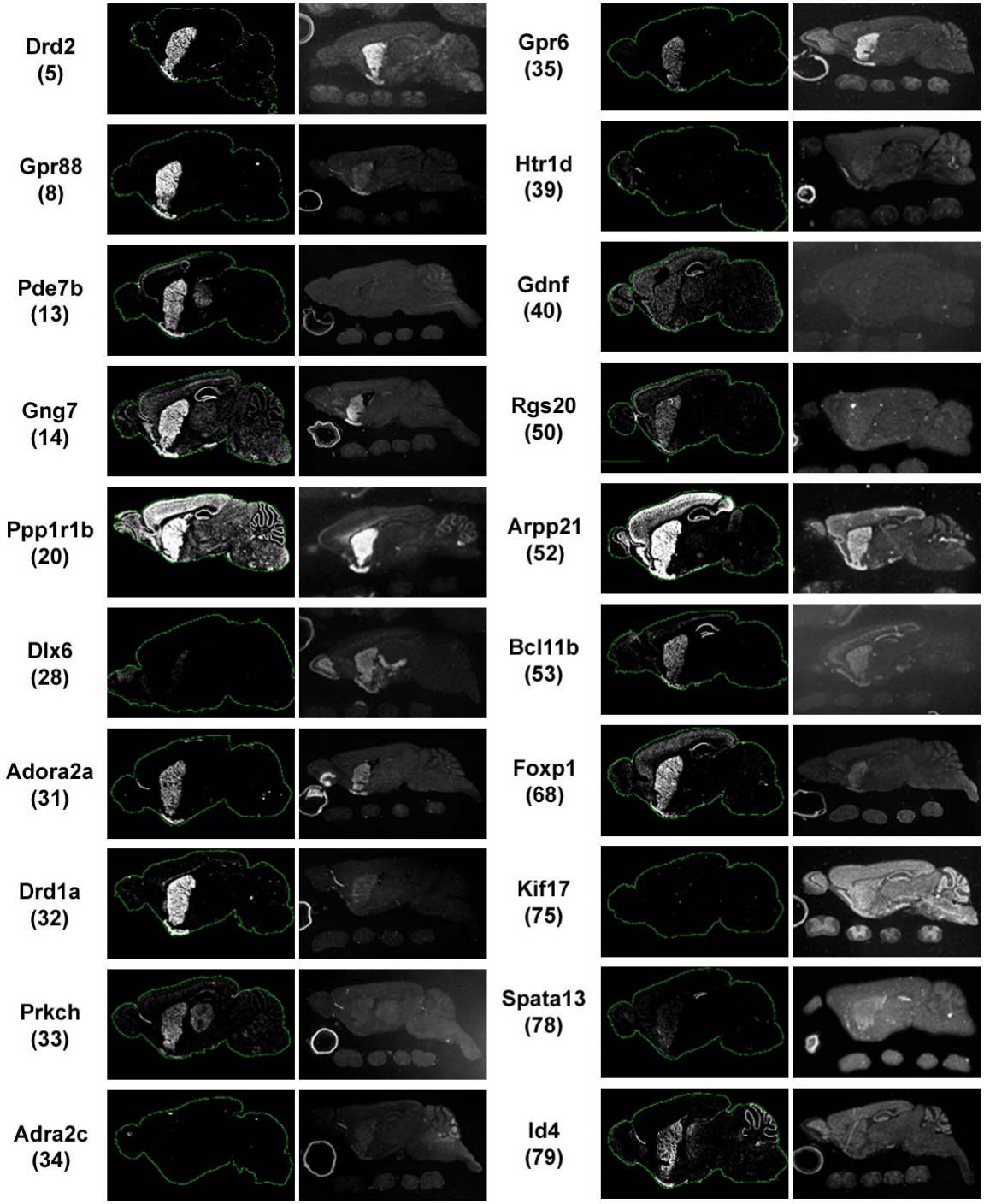

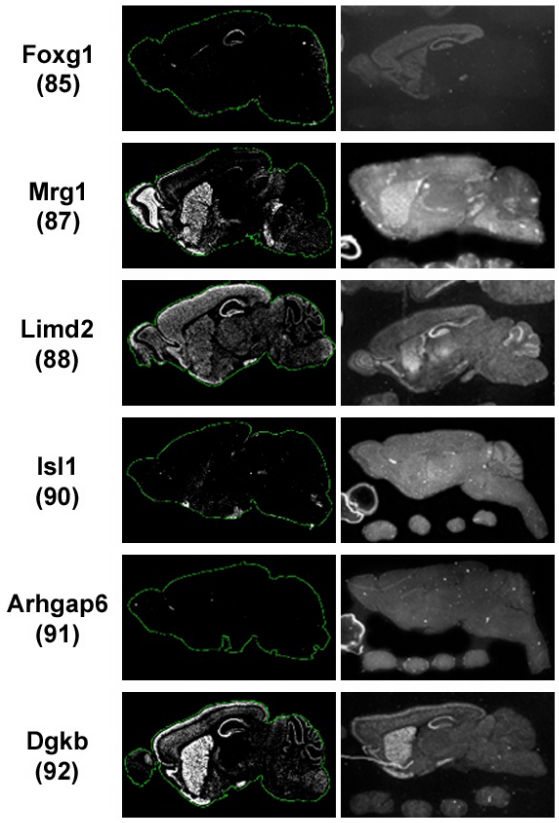

Figure S5. Expression analysis of medium spiny neuron (MSN)-enriched genes
Expression analysis in sagittal sections of genes which were amongst the top 100 genes identified in our study as MSN-enriched, with the rank order of each gene noted below the gene name. Non-redundant gene ranking was calculated using the highest-ranked probeset corresponding to each gene (Table S5), with redundant probesets eliminated. Left panel, *in situ* hybridization images taken from the Allen Brain Atlas (Allen Brain Atlas [Internet]. Seattle (WA): Allen Institute for Brain Science. © 2006. Available from: http://www.brain-map.org.) (Lein et al., 2007); right panel, *in situ* hybridization images taken from the Brain Gene Expression Map (BGEM) database (http://www.stjudebgem.org/) (Magdaleno et al., 2006). Allen Brain Atlas images all correspond to adult brain; BGEM images all correspond to adult brain except for the following, for which the oldest available data was postnatal day 7 (P7): *Drd2*, *Ppp1r1b*, *Dlx6*, *Gdnf*, *Bcl11b*, *Foxg1*, *Limd2*.

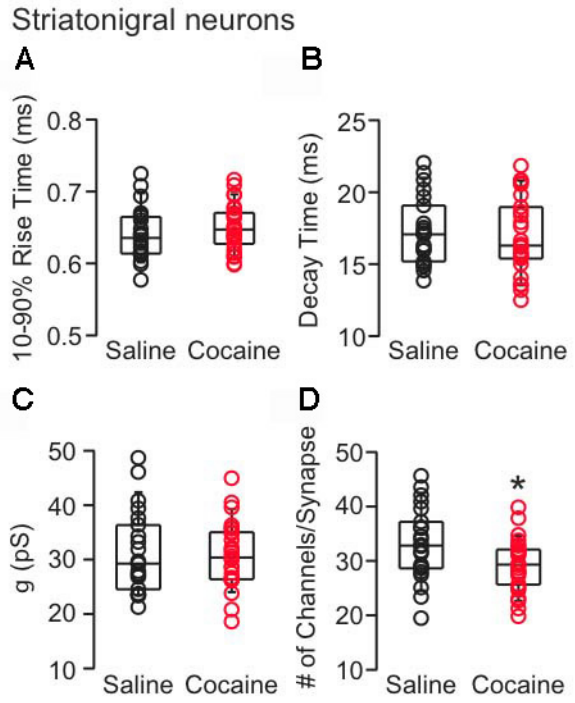

Figure S6. Cocaine treatment decreases the number of $GABA_A$ channels per synapse in BAC *Drd1a* striatonigral neurons. Box plot summaries showing mean mIPSCs kinetics and non-stationary noise analysis measures of individual striatonigral neurons taken from saline-treated control and 15-day treated cocaine BAC *Drd1a* mice. (A) Neither mean 10-90% rise times (one-tailed t-test, $p>0.05$, Saline=0.64±0.008, n=22; Cocaine=0.65±0.006, n=26) nor (B) mean decay times (one-tailed t-test, $p>0.05$, Saline=17.3±0.5, n=22; Cocaine=17.0±0.5, n=26) were significantly different between groups. Non-stationary noise analysis of mIPSCs demonstrated no change between groups in the (C) mean unitary conductance (γ) of $GABA_A$ receptors of striatonigral neurons (one-tailed t-test, $p>0.05$, Saline γ=31.1±1.6, n=22; Cocaine γ=30.8±1.2, n=26), and a significant decrease in the (D) mean number of channels per synapse in striatonigral neurons taken from cocaine treated BAC *Drd1a* mice (one-tailed t-test, $p<0.05$, Saline N=33.1±1.4, n=22; Cocaine N=29.3±1.0, n=26).

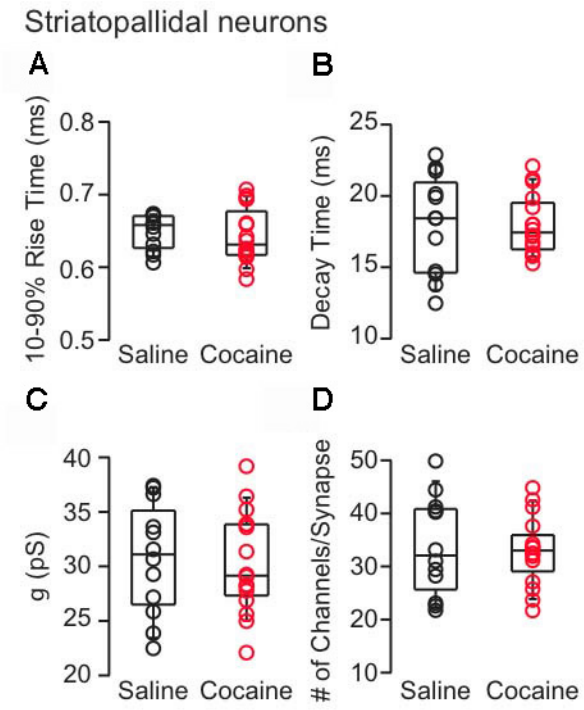

Figure S7. Cocaine treatment does not alter GABAergic mIPSCs kinetics or $GABA_A$ receptor number per synapse or unitary receptor conductance in BAC *Drd2* striatopallidal neurons. Box plot summaries showing mean mIPSCs kinetics and non-stationary noise analysis measures of individual striatopallidal neurons taken from saline-treated control and 15-day treated cocaine BAC *Drd2* mice. (A) Neither mean 10-90% rise times (one-tailed t-test, $p>0.05$, Saline=0.65±0.007, n=12; Cocaine=0.64±0.010, n=16) nor (B) mean decay times (one-tailed t-test, $p>0.05$, Saline=18.0±1.0, n=12; Cocaine=18.0±0.5, n=16) were significantly different between groups. Non-stationary noise analysis of mIPSCs demonstrated no change between groups in the (C) mean unitary conductance (γ) of $GABA_A$ receptors of striatopallidal neurons (one-tailed t-test, $p>0.05$, Saline=30.7±1.5, n=12; Cocaine=30.3±1.2, n=16) or in the (D) mean number of channels per synapse in striatopallidal neurons taken from cocaine treated BAC *Drd2* mice (one-tailed t-test, $p>0.05$, Saline N=33.8±2.7, n=12; Cocaine N=33.0±1.6, n=16).

Note: Tables S2 and S5 through S26 are stand-alone spreadsheet items.

Table S1. Total RNA yields from cultured cell TRAP purifications HEK293T cells were transiently transfected with EGFP (mock transfection) or EGFP-L10a constructs. Transfection efficiency was approximately 30%. Plates of different sizes were used to grow mock or EGFP-L10a-transfected cells, which is reflected in different input RNA amounts. Input and immunoprecipitated (bound) RNA were purified and the quantity and purity of RNA were determined using a Bioanalyzer 2100 (Agilent Technologies).

Transfection	Total RNA Bound (ng)	Total RNA in Input (ng)	Yield (%)
EGFP (Mock)	61	33,320	0.2
EGFP-L10a	6,117	56,630	10.8

Table S3. Real-time PCR analysis of *Drd1a*-enriched messages: range from replicates

Gene	Fold enrichment in *Drd1a* versus *Drd2* cell type
Eya1	19.85 - 21.51
Tac1 (known)	10.97 - 11.87
Isl1	10.06 – 10.87
Gng2	5.91 – 6.43
Chrm4 (known)	5.02 – 5.57
Drd1a (known)	2.96 – 3.4
Crym	1.57 – 1.88

Table S4. Real-time PCR analysis of *Drd2*-enriched messages: range from replicates

Gene	Fold enrichment in *Drd2* versus *Drd1a* cell type
Drd2 (known)	49.79 - 51.55
Gpr6	12.30 – 12.81
Lhx8	3.57 – 4.06
Gpr88	1.94 – 2.13
Trpc4	1.93 – 2.25
Tpm2	1.84 – 1.96

Supplemental References

Alexa, A., Rahnenfuhrer, J., and Lengauer, T. (2006). Improved scoring of functional groups from gene expression data by decorrelating GO graph structure. Bioinformatics *22*, 1600-1607.

Doyle, J.P., Dougherty, J.D., Heiman, M., Schmidt, E.F., Stevens, T.R., Ma, G., Bupp, S., Shrestha, P., Shah, R.D., Doughty, M.L., et al. (2008). Application of a translational profiling approach for the comparative analysis of CNS cell types. Cell *135*, this issue.

Falcon, S., and Gentleman, R. (2007). Using GOstats to test gene lists for GO term association. Bioinformatics *23*, 257-258.

Gaspar, P., Bloch, B., and Le Moine, C. (1995). D1 and D2 receptor gene expression in the rat frontal cortex: cellular localization in different classes of efferent neurons. Eur J Neurosci *7*, 1050-1063.

Gong, S., Zheng, C., Doughty, M. L., Losos, K., Didkovsky, N., Schambra, U. B., Nowak, N. J., Joyner, A., Leblanc, G., Hatten, M. E., and Heintz, N. (2003). A gene expression atlas of the central nervous system based on bacterial artificial chromosomes. Nature *425*, 917-925.

Lein, E. S., Hawrylycz, M. J., Ao, N., Ayres, M., Bensinger, A., Bernard, A., Boe, A. F., Boguski, M. S., Brockway, K. S., Byrnes, E. J.*, et al.* (2007). Genome-wide atlas of gene expression in the adult mouse brain. Nature *445*, 168-176.

Magdaleno, S., Jensen, P., Brumwell, C. L., Seal, A., Lehman, K., Asbury, A., Cheung, T., Cornelius, T., Batten, D. M., Eden, C.*, et al.* (2006). BGEM: an in situ hybridization database of gene expression in the embryonic and adult mouse nervous system. PLoS Biol *4*, e86.

Rogers, J., and Munro, H. (1987). Translation of ferritin light and heavy subunit mRNAs is regulated by intracellular chelatable iron levels in rat hepatoma cells. Proc Natl Acad Sci U S A *84*, 2277-2281.

Smyth, G. K. (2004). Linear models and empirical bayes methods for assessing differential expression in microarray experiments. Stat Appl Genet Mol Biol *3*, Article3.

Suarez-Farinas, M., Pellegrino, M., Wittkowski, K. M., and Magnasco, M. O. (2005). Harshlight: a "corrective make-up" program for microarray chips. BMC Bioinformatics *6*, 294.

Zahringer, J., Baliga, B. S., and Munro, H. N. (1976). Novel mechanism for translational control in regulation of ferritin synthesis by iron. Proc Natl Acad Sci U S A *73*, 857-861.